LAWRENCE
LIVERMORE
NATIONAL
LABORATORY

UCRL-JRNL-217359

Fabrication and Characterization of Graded Impedance Gas Gun Impactors from Tape Cast Metal Powders

L. P. Martin, J. H. Nguyen

November 29, 2005

Materials Science and Engineering, A

Fabrication and Characterization of Graded Impedance Gas Gun Impactors from Tape Cast Metal Powders

L. Peter Martin* and Jeffrey H. Nguyen

Lawrence Livermore National Laboratory, Mail code: L-353

P.O. Box 808, Livermore, CA 94551

*Corresponding author: Phone: 925-423-9831, Fax: 925-423-7040, email: martin89@llnl.gov

ABSTRACT

Fabrication of compositionally graded structures for use as light-gas gun impactors has been demonstrated using a tape casting technique. Mixtures of metal powders in the Mg-Cu system were cast into a series of tapes with uniform compositions ranging from 100% Mg to 100% Cu. The individual compositions were fabricated into monolithic pellets for characterization by laminating multiple layers together, thermally removing the organics, and hot-pressing to near-full density. The pellets were characterized by optical and scanning electron microscopy, X-ray diffraction, and measurement of density and sound wave velocity. The density and acoustic impedance were observed to vary monotonically (and nearly linearly) with composition. Graded structures were fabricated by stacking layers of different compositions in a sequence calculated to yield a desired acoustic impedance profile. The measured physical properties of the graded structures compare favorably with those predicted from the monolithic-pellet characteristics. Fabrication of graded impactors by this technique is of significant interest for providing improved control of the pressure profile in gas gun experiments.

Keywords: Magnesium, copper, tape cast, acoustic impedance, sound wave velocity.

INTRODUCTION

Investigation of material properties at extreme conditions, e.g., megabar pressures and/or thousands of degrees in temperature, is of interest in fields as diverse as biology, condensed matter physics, and planetary sciences.[1-5] Various experimental techniques have been developed over the past several decades to achieve these conditions. These include quasi-static measurements using diamond anvil cells [6], shock compression techniques [7], and quasi-isentropic compression techniques.[8,9,10] Recently, experimental techniques enabling quasi-isentropic compression during light-gas gun experiments have generated growing interest.[11-17] In particular, it has been proposed that the use of a layered (normal to the propagation direction) impactor may enable increased flexibility in designing applied-pressure profiles through various combinations of shock, quasi-isentropic compression, controlled release, and constant pressure, thus relieving constraints on the thermodynamic path.[11,12] This means that the evolution of the pressure experienced by the target material can be 'tailored' by appropriately designing the density, or rather the shock impedance, profile through the thickness of the impactor. However, the nature of these gas gun experiments, especially the very short time scales involved, place stringent requirements on the uniformity, planarity, and overall quality of the layered impactor.[1]

Various techniques have been reported for fabricating graded impactors for light-gas gun experiments. These include diffusion bonding solid plates [13,18] and hot-pressing powder compacts.[11-14,19] The diffusion bonding technique has the potential to provide high quality impactors, however the resultant profiles are limited by the layer thickness and the number of layers which can realistically be incorporated, and by the diffusion characteristics at each interface. Also, extremely smooth and flat surfaces are required on each of the layers to achieve

the intimate contact necessary for the diffusion bonding, which tends to make the fabrication cost prohibitive. Techniques based on powder processing are attractive because they have the potential to provide essentially continuously variable properties (i.e., density, impedance) based on the powder composition. Dense impactors are fabricated by loading the constitutive powders into a die and applying elevated temperature and pressure. The composition of the powder can be varied as a function of depth either prior to, or during, loading of the powder into the die to achieve the desired gradient in the final properties. The method is simple in principle, however accurate layering of the different powder compositions can be tedious and time consuming, and the spatial uniformity of the profile can be sensitive to numerous aspects of the process including: operator error, friction at the mold wall, segregation of the powders during handling, and even ambient humidity levels.

Tape casting has been widely applied to the fabrication of functionally graded materials for various applications.[20,21,22] In tape casting, a powder is mixed into an organic solvent with suitable plasticizers and binders to form a slurry (or 'slip') with a viscosity in the range of 500-6000mPa·s. The slip is then cast onto a mylar carrier film to form a tape which can range from several μm to a few mm in thickness. After a drying process, which removes the residual solvent, the resultant tape is smooth and flexible, and can be easily handled, cut or punched. Multiple layers of the tape can be laminated together with the application of slightly elevated temperature (50-200^{o}C) and pressure (3-30MPa). Laminating tapes with different compositions provides a convenient route to fabricating a graded, or tailored, profile through the thickness of the laminate. Final processing of the laminate involves removing the organic binders at elevated temperature, and hot-pressing to full density.

In the present work, tape casting is demonstrated to be an effective route to fabrication of

functionally graded impactors for quasi-isentropic light-gas gun experiments. A prototype series of seven tapes in the Cu-Mg system is prepared and characterized. The lamination, binder removal, and hot-pressing procedures are discussed. The final density, thickness, sound wave velocity, and acoustic impedance are determined for each composition. A series of graded laminates are fabricated from layers of these compositions with the intent to match impedance profiles suitable for the aforementioned light-gas gun experiments.

MATERIALS AND METHODS

Tape casting – A series of Cu-Mg powder mixtures were cast into tapes for evaluation and, ultimately, for graded impactor fabrication. The tape casting was performed by a commercial vendor (Maryland Ceramic & Steatite, Bel Air, MD). Table I lists the relative volume fractions of Cu and Mg powders used in the seven tapes which were cast for this investigation. It can be seen that, once fully densified, the compositions are intended to span the range of density from Mg (1.74g/cm^3) to Cu (8.93g/cm^3) in a series of discrete steps. Commercially available, -325 mesh, Cu (Alfa Aesar, 13990) and Mg (Alfa Aesar, 10233) powders were used for the tape casting process. Methyl methacrylate:ethyl acrylate and dibutyl phthalate were used for the binder and plasticizer, respectively, because they are known to depolymerize at elevated temperature. This facilitates subsequent organic removal (discussed below) by heating in an inert atmosphere, rather than by 'burning out' in air as is customary when casting oxide powders. This capability is important because oxidation of the metal powders during organic removal in air is known to inhibit densification during the subsequent hot-pressing step.[23] Composition ranges for the organics used in the tapes are listed in Table II. The organic content varies as a function of the composition of the metal powder mixture due to the different particle size,

specific surface area, and density of the Cu and Mg powders.

The steps of the tape casting process are illustrated schematically in Fig. 1. The powders are ball milled for 24 hours in MEK, with a dispersant, to ensure wetting of the powders, break-up of particle agglomerates, and complete mixing of the powders. The binder and plasticizer are added, and a second milling step is performed to insure complete mixing of those components. The resultant mixture, is de-aired and filtered, cast onto a moving mylar carrier, then dried overnight. In this work, casting was performed with a blade gap of 0.23mm at a speed of 8.5mm/s, and drying was performed at room temperature. Cast tapes had bulk 'green' densities of 0.98 – 3.97g/cm^3, and thickness of 78.7 – 104.1μm.

Lamination, organic removal, and hot-pressing – Cast tapes were laminated to form cylindrical pellets on the order of several mm thick for characterization, and to fabricate prototype graded impedance impactors. Discs with a diameter of 31mm were punched from the tapes and stacked inside a right cylindrical die with a matching inside diameter. For characterization of the individual tapes, 20 layers of a single tape are laminated to form a pellet. For fabrication of graded impedance impactors, multiple layers of different tapes are laminated together, and the stacking sequence is determined by calculating the best fit to the desired impedance profile based on the characterization of the individual-tape pellets. Once placed in the die, the stacked tapes are laminated by heating the die assembly in N_2 to an internal temperature of 75^{o}C, and applying a pressure 16.8MPa for 5 minutes. The laminate is subsequently extracted from the die, and the organics are removed by (pressureless) heating at 1^{o}C/min to 350^{o}C in flowing N_2, with intermittent dwells at 150 and 250^{o}C, and holding for 3 hours.

After the organics are removed, the laminated pellet is returned to the die, and hot-

pressed for one hour, in air, at 375°C and 225MPa. The pressing temperature is kept intentionally low in order to minimize the formation of unwanted intermetallic phases, Mg_2Cu and $MgCu_2$, and as a result it can be performed in air without significant oxidation of the metal powders. These issues will be discussed in more detail below. During fabrication of the graded impactors, cooling is performed under load in order to constrain sample deformation ('warping') resulting from the thermal expansion mismatch between layers with differing compositions.

Materials characterization - The organic materials used for tape casting were characterized by thermogravimetric analyses (TGA) in order to identify an effective organic removal procedure (Shimadzu, TGA-50). The analyses were performed in flowing N_2 using an Al_2O_3 sample pan. The sample chamber was pumped down to <200mTorr and backfilled with dry N_2 several times prior to establishing the N_2 flow and initiating the thermal cycle. TGA data for the organic removal cycle are shown in Fig. 2, where it can be seen that there is complete removal of the plasticizer (curve a). In contrast, the dispersant (curve b) and binder (curve c) leave ~4.5% and 0.6% by weight, respectively, of carbonaceous residue. Based on the ranges of organic content used in the tapes, Table II, this implies a maximum of ~0.086% by weight of residue from the organic removal process.

After hot pressing, single-tape laminates were evaluated by x-ray diffraction (XRD) for the formation of oxide and intermetallic phases using Cu K_α radiation and an analyzing graphite crystal at 40 kV (Phillips, APD3720). Step scans were performed from 30-100° with a 0.02° step size and 2-s counting period. Samples were prepared for the XRD by lapping the surface with 600-grit SiC sandpaper to ensure flatness and to remove any surface contamination which might be present. Density of the hot-pressed pellets was calculated from the mass, diameter and

thickness. Past experience indicates that this technique is accurate to within 1.5% relative to the Archimedes method, and reduces the potential for infiltration of fluid into any residual, surface-breaking porosity. Thickness was determined by averaging multiple measurements, made with a micrometer, at the center and around the perimeter. For each tape composition, the hot-pressed (final) thickness of a single layer was determined from the ratio of the thickness and the number of layers in the pellet.

Contact ultrasonic measurements were performed on the single-tape pellets using a 50MHz compressional wave contact transducer. The transducer emits ultrasonic sound waves into the sample when excited by a pulse from an ultrasonic pulser-receiver (Panametrics, 5800), and monitors the reverberations of these sound waves as they echo between the free surfaces of the sample. The time of flight required for the sound waves to pass through the sample was determined by the pulse-echo overlap method on a digital oscilloscope. The compressional sound wave velocity, V_L, is determined from

$$V_L = \frac{2l}{t_{pe}} \tag{1}$$

where l is the thickness, and t_{pe} is the pulse-echo' time of flight. The factor of 2 appears because the pulse-echo time of flight is, by definition, the time required for the sound waves to travel though the sample twice, i.e. from the transducer to the opposite surface and back. The (ambient pressure) compressional wave acoustic impedance, r_L, is

$$r_L = r \cdot V_L \tag{2}$$

where r is the bulk density.

Optical microscopy was performed on a polished cross-section of a graded impactors to evaluate the microstructure after densification. The cross-section was polished down to 0.04μm

SiO_2 in a kerosene solution. The polished cross-section was also inspected by scanning electron microscopy (SEM), as were fracture surfaces of selected single-composition pellets.

RESULTS AND DISCUSSION

Fig. 3 shows the density and layer thickness as a function of composition for pellets fabricated from the tape cast Cu-Mg powder mixtures. The data are also summarized in Table I. For each of the seven tape compositions, 20 layers were laminated together and densified by the procedure described above. The final densities can be seen to vary linearly with composition. A least squares regression fit, shown as a solid line in Fig. 3, yields an R^2 value of 0.997. A linear mixing law given by

$$r_{mix} = X_{Cu} r_{Cu} + (1 - X_{Cu}) r_{Mg}, \qquad (3)$$

where X_{Cu} is the volume fraction of Cu, and r_{Cu} and r_{Mg} are the theoretical densities of Cu and Mg, respectively, is also shown as a dotted line in Fig. 3. Eq. (3) assumes that the end product is a fully dense composite of Mg and Cu, neglects any alloying, oxidation, or reaction of the Mg and Cu, and is the basis for the compositionally dependant theoretical densities cited in Table I. A slight deviation of the measured densities from those predicted by Eq. (3) is observed in Fig. 3. At the 100% Cu composition, the density is slightly low due to the presence of ~4% by volume residual porosity. At the intermediate compositions, the measured and predicted densities are very close, in most cases agreeing to within the experimental uncertainty of the density measurements. At the lowest Cu compositions, MC-6 and MC-7, the measured densities fall somewhat above those predicted by Eq. (3) due, in part, to the slight oxidation of the Mg powder to MgO, which has a higher density than Mg (3.84 vs. 1.74g/cm^3, respectively). Obviously, this effect is most pronounced for the compositions with the highest Mg content. In addition, the

100% Mg (0% Cu) composition was inadvertently contaminated with W powder due to a processing error, yielding a slight additional increase in density.[24] These issues will be discussed in more detail below.

Also shown in Fig. 3 are the layer thicknesses for each tape cast composition. These thicknesses represent the ratio of the full thickness of each (hot pressed) pellet and the number of tape cast layers contained therein (20). Thus, each composition of tape can be expected to yield a single layer (or multiple layers) of the specified thickness when incorporated into either a single-composition pellet or into a graded impactor. Knowledge of these layer thicknesses, which are also tabulated in Table I, allows accurate control of the density/impedance gradients when fabricating graded impactors from these tapes. Fig. 3, and Table I, show that the layer thicknesses are fairly consistent between compositions, all falling between 33.8 and 44.4μm. It should be noted that these ultimate thicknesses are a strong function of the tape casting process including, especially, the viscosity of the slip from which the tapes are cast. This viscosity is, in turn, a strong function of the solids loading (i.e. how much metal powder vs. solvent), and the interaction of the powder surfaces with the dissolved organics. Because there is a complex interplay between powder characteristics (most notably surface area) and the slip behavior, the formulation must be adjusted as a function of the powder mixture in order to maintain a castable consistency. The net effect is a 'learning' curve whereby the expectation is that future casting runs will yield even more consistent results.

Figures 4 and 5 show SEM micrographs of fracture surfaces from the 100% Cu and Mg compositions, respectively. These images are oriented such that the force applied during hot pressing was in the vertical direction. Figure 4 shows the Cu microstructure to be near full density. Some residual porosity is apparent in the lower magnification image, which is

consistent with the measured density (8.55g/cm^3). No signs of macroscopic defects, such as voids or interlayer delamination, were observed. Similarly, the Mg microstructure shown in Figure 5 appears to be near full density. There is some evidence of cracking, which is attributed to the process of fracturing the sample for inspection. Widely scattered W particles, per the contamination discussed above, were observed to have a nominal particle size <1μm.

XRD was performed in order to evaluate the phase purity of the densified powder mixtures. Of particular interest, given that the processing is performed in air, is the formation of oxides of Mg and/or Cu. Fig. 6 shows the XRD patterns for the 100% Mg (upper) and Cu (lower) compositions, MC-1 and MC-7 in Table I. The lower curve shows only the diffraction peaks for Cu, indicating that any oxide formation is limited to a level below the detection threshold of the XRD. The upper curve shows, in addition to the pattern for Mg, several peaks which are consistent with the presence of a small amount of W. In addition, there is a weak, diffuse peak at ~42.9^o which is consistent with the strongest peak in the MgO diffraction pattern. For the experimental technique used to generate these XRD data, the detection limit is expected to be in the range of ~5-8%. Based on this, the volume fraction of Mg which can be inferred to have oxidized to MgO is consistent with the measured densities given in Table I.

Having determined oxidation effects to be negligible for the proposed application, it is also of interest to evaluate the formation of additional phases formed by the direct reaction of the Mg and Cu powders. Mg and Cu are known to have two intermetallic phases $MgCu_2$ and Mg_2Cu.[25,26] The compositions of MC-3 and MC-5, from Table I, were intentionally selected to correspond to the stoichiometries of these two phases. Figs. 7a-c show the XRD patterns for dense pellets fabricated from these compositions. Fig. 7a shows the pattern for the MC-5 composition, which corresponds to 67 atomic % Mg and 33 atomic % Cu. The pattern is

dominated by the peaks for Mg and Cu, with visible peaks from both Mg_2Cu and $MgCu_2$. The XRD pattern for the MC-3 composition, corresponding to 67 atomic % Cu and 33 atomic % Mg, is shown in Fig. 7b and yields a qualitatively similar result albeit with a smaller contribution from the intermetallic phases. It is interesting to note the formation of both intermetallic phases at both compositions. Fig. 7c shows an expanded view of this region from Figs. 7a and b. The upper curve in Fig. 7c is from the MC-5 composition, while the lower curve is from MC-3. For both compositions, peaks at 37.3 and 39.5^o are definitively attributable to the Mg_2Cu phase, while the peak at 42.6^o is unambiguously attributable to $MgCu_2$. Both phases have a peak at 44.6^o, making that feature impossible to assign to either phase. Figs. 7a and b show that the formation of the intermetallic phases is only slight, and occurs preferentially in the Mg-rich compositions. XRD performed on other compositions yielded qualitatively similar results.

Reported densities for the two intermetallics (Mg_2Cu: 3.18g/cm^3 and $MgCu_2$: 5.72g/cm^3 [27]) deviate by <8% from the densities predicted by Eq. (3) for those compositions, given in Table I as 3.19g/cm^3 and 5.31g/cm^3. In addition, the elastic moduli of Mg-Cu mixtures have been reported to vary linearly from Mg up to the saturated Cu solid solution (97.23 weight % Cu) regardless of the formation of the two intermetallic phases.[25] The expectation is, therefore that the slight intermetallic formation observed in the XRD data does not pose a significant concern with respect to maintaining a smooth compositional dependence of the elastic moduli. This leads to the additional expectation that the sound wave velocity, and hence the acoustic impedance, should also vary smoothly as a function of composition.

Fig. 8 shows the compressional sound wave velocity and acoustic impedance as a function of volume % Cu for monolithic pellets fabricated by hot-pressing the tape cast Cu-Mg powder mixtures. The data show sound wave velocities of 5.539 and 4.307mm/μs for the

terminal (100%) Mg and Cu compositions, respectively. These compare favorably with published values for these materials (Mg: 5.77 – 6.31mm/μs and Cu: 4.70 – 4.66mm/μs).[28,29] Deviations from the published values are attributed to low levels of residual porosity in the Cu, and to the aforementioned W and MgO impurities in the Mg. It is well known that the inclusion of small amounts of a secondary phase, especially porosity, can substantially alter sound wave velocity.[30,31] Fig. 8 also shows that the compositional dependence of the sound wave velocity has a pronounced minimum at ~50% Cu. While the compositional dependence of velocity in multi-phase media can be difficult to predict quantitatively due to a strong dependence on microstructural features such as the size and shape of the dispersed phase(s), theoretical bounds can be expressed based on various models. It is worthwhile here to consider the compositional dependence of the measured sound wave velocities within the context of certain models describing the variation of the elastic moduli with composition.

The models of Voight (constant strain) and Reuss (constant stress) are widely cited as providing upper and lower bounds for the compositional dependence of the elastic moduli in two phase media.[30,32,33] These bounds can be expressed as

$$\text{Voight:} \qquad E_V = E_2 f_2 + E_1(1 - f_2) \tag{4}$$

$$\text{Reuss:} \qquad E_R = \frac{E_1 E_2}{E_1 f_2 + E_2(1 - f_2)} \tag{5}$$

where E_i and f_i are the elastic modulus and volume fraction of component I, respectively. Given the assumption of linear elastic behavior, generally valid for metallic materials given the small strains associated with the ultrasonic measurements (=10^{-4}), the elastic modulus and sound wave velocity are related by

$$E = V^2 r \tag{6}$$

where V is the sound wave velocity and r is the density. Eq.'s (4) and (5) are generalized expressions which are not dependant upon which modulus is of interest (i.e. bulk, shear, Young's, etc.). In Eq. (6), the modulus is determined by the mode of propagation used to determine V (i.e., compressional, transverse). In our case, V represents V_L, the compressional (or 'longitudinal') sound wave velocity, and yields for E the so-called longitudinal modulus. While this modulus is not directly of interest, it can be used to apply the Voight and Reuss expressions to bound the compressional velocity by substituting the endpoint densities and velocities (100% Cu and 100% Mg) from Figs. 3 and 8 into Eq. (6), using the resultant moduli to calculate E_V and E_R as a function of composition, and then applying Eq. (6) to convert the calculated moduli back to compressional velocities using the measured compositionally-dependant densities shown in Fig. 3. The results of these calculations are also shown in Fig. 8, where it can be seen that the minimum in the velocity, which occurs at intermediate compositions, is predicted by the Reuss model a natural and expected consequence of approaching a condition of equal stress in the two phases. It should be noted that application of these data to calculating the Voight and Reuss bounds is not strictly correct since it does not account for the small amounts of additional phases which might be present (porosity, MgO, etc.). The calculation is provided, however, only with the intent of phenomenologically demonstrating that the observed minimum in the compositional dependence falls within the expected range of behavior for a (nominally) two-phase mixture.

The values of sound wave velocity, Fig. 8, and density, Fig. 3, were substituted into Eq. (2) to calculate the (ambient pressure) compressional wave acoustic impedance. This is shown in Fig. 8 to vary from 10.7-36.8 $x10^6 kg/m^2 s$. These acoustic impedances were used to design a graded, or rather 'stepped', impedance impactor. The target impedance profile, shown as the solid line in Figure 9, was designed to provide an initial shock loading, followed by a relatively

'slow' (hundreds of ns) compression, in an Al target. The impedance and thickness data discussed above were used to design a stacking sequence for the tapes that would most closely follow the target profile. This sequence is also shown in Figure 9, where each symbol (?) represents the end of a single layer. The stacking sequence also includes ~250 and ~500 μ m excess on the low and high impedance ends, respectively. These 'runouts' are included to facilitate validation of the impactor performance by providing constant, known states at the beginning and end of the gas gun experiment.

Figure 10 shows optical and SEM micrographs of a polished cross section from the graded impactor. These images show excellent planarity and parallelism between the layers. The composition gradient ranging from Cu (bottom) to Mg (top) is clearly visible in both images. In the optical micrograph, Fig. 10a, the Mg phase presents a mottled appearance due to significant polishing artifacts, most of which appear to be pullouts. In the SEM image, Fig. 10b, there is clear evidence that the Mg phase has been polished more deeply than the Cu (i.e., the Cu particles present a higher surface). This differential polishing makes it difficult to interpret the details of the microstructure, for example feature dimensions, with any certainty. Ongoing work will further evaluate the spatial distribution of the Mg and Cu within the individual layers.

It should be noted that the reproducibility of graded impactors fabricated by this technique is quite good. Table III shows a comparison of the measured thickness, mass, density, sound wave velocity, and acoustic impedance, as a percentage of the predicted values, for a series of graded impactors prepared from the tape cast Cu-Mg powders. The predicted values are determined from the measured properties of the individual compositions, discussed above, and the sequence in which the tapes were stacked to form the impactor. Note that for impactor #4 in the Table, a single layer was left out during the fabrication process, and the resultant decrease in

mass is readily apparent. For the other impactors, the measured and predicted values agree to within 2.5% in the worst case (thickness) and in most cases to within ~1%. In the case of the thickness, this means that the fabricated impactor matches the predicted thickness to within ~55μm out of a full thickness of >2mm. In addition, the faces of the impactors are parallel to within 0.32±0.1mrad, and are flat to within 0.08±0.04%. Gas gun experiments are currently in progress to evaluate graded impactors fabricated form this methodology. In addition, the technique is in the process of being further refined to allow significantly better control over the impedance profile, and impactor quality and repeatability.

CONCLUSIONS

Fabrication of compositionally graded structures for use as light-gas gun impactors has been demonstrated using a tape casting technique. Mixtures of metal powders in the Mg-Cu system were cast into a series of tapes with uniform compositions ranging from 100% Mg to 100% Cu. The individual compositions were fabricated into monolithic pellets for characterization by laminating multiple layers together, thermally removing the organics, and hot-pressing to near-full density. The pellets were characterized by optical and scanning electron microscopy, X-ray diffraction, and measurement of density and sound wave velocity. The microscopy shows near dense microstructures at all compositions. The XRD indicates the formation of low levels of MgO, Mg_2Cu and $MgCu_2$ at certain compositions. However, based on the density and acoustic impedance, which were observed to vary monotonically (and nearly linearly) with composition, the presence of these levels of the secondary phases does not impact the current application. Graded structures were fabricated by stacking layers of different compositions in a sequence calculated to yield a desired acoustic impedance profile. The

measured physical properties of the graded structures, such as density and thickness, compare favorably with those predicted from the monolithic-pellet characteristics. Fabrication of graded impactors by this technique is of significant interest for providing improved control of the pressure profile in gas gun experiments.

ACKNOWLEDGMENTS

The authors which to thank Ernest Bianchi at Maryland Ceramic and Steatite for tape casting services. Thanks also to Gary Freeze, Pat Roberson and Leon Berzins of Lawrence Livermore National Laboratory. This work was performed under the auspices of the U. S. Department of Energy by the University of California, Lawrence Livermore National Laboratory under Contract No. W-7405-Eng-48.

Table I: Composition and final (hot-pressed) density for the tape cast Mg – Cu powder mixtures. Also shown are the 'theoretical' densities predicted by Eq. (3), and the layer thickness for each tape composition.

Tape designation	% Mg, by volume	% Cu, by volume	Measured density, g/cm^3	Theoretical density, g/cm^3	Thickness, mm
MC-1	0.0	100.0	8.55 ±0.13	8.93	37.5
MC-2	31.6	68.4	6.73 ±0.10	6.66	33.8
MC-3	50.3	49.7	5.47 ±0.082	5.31	34.1
MC-4	68.7	31.3	4.00 ±0.060	3.99	37.0
MC-5	79.8	20.2	3.25 ±0.048	3.19	41.4
MC-6	92.9	7.1	2.43 ±0.038	2.25	44.4
MC-7	100.0	0.0	1.93 ±0.029	1.74	39.0

Table II: Typical organic content for tape cast Mg – Cu powder mixtures. Specific formulations are dependant upon the density and specific surface area of the powder solids.

Component	Function	Weight %
Hypermer KD-1	Dispersant	0.40 – 0.62
MEK	Solvent	10.8 – 30.1
Dibutyl Pthalate	Plasticizer	1.24 – 1.74
Ethyl methacrylate copolymer	Binder	7.33 – 9.65
Cu + Mg powder	Solids	57.9 – 79.2
Total organic	-	10.9 – 17.1*
Metal powder	-	82.9 – 89.1*

* Discludes solvent.

Table III: Measured characteristics of several graded impactors fabricated from the tape cast Mg - Cu powder mixtures. Values are expressed as the percentage of that predicted from the stacking sequence (Fig.) and the individual tape characteristics.

Impactor	Thickness	Mass	Density	Velocity	Impedance
1	97.63	98.91	101.58	98.99	100.55
2	97.50	98.08	100.87	99.34	100.20
3	98.03	98.76	101.02	99.00	100.01
4*	96.64	96.97	100.62	98.85	99.47
5	100.07	99.64	99.73	**	**
6	99.39	100.0	99.88	**	**
7	99.39	100.0	99.88	**	**

* One layer, out of a total of 50, was left out during fabrication.
** Not measured.

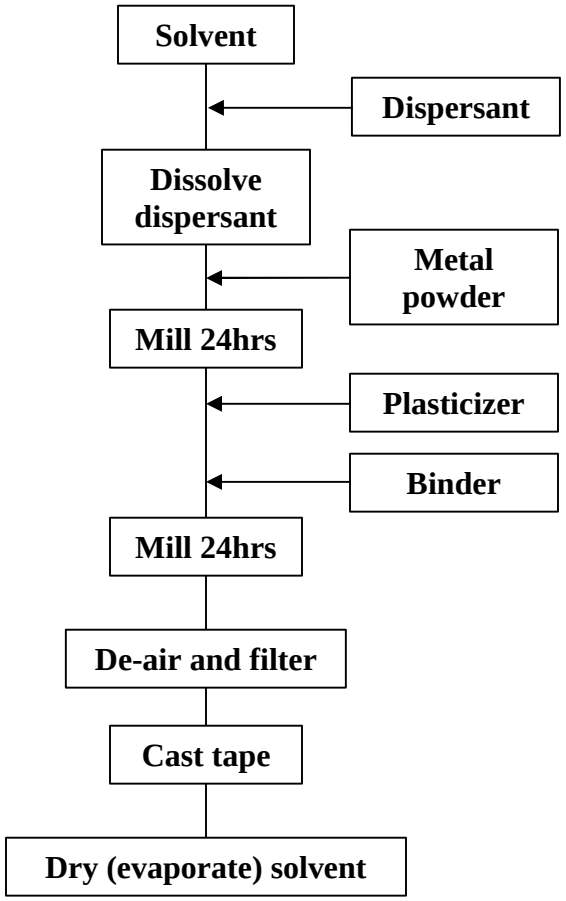

Figure 1: Flow chart illustrating the steps in a typical tape casting process.

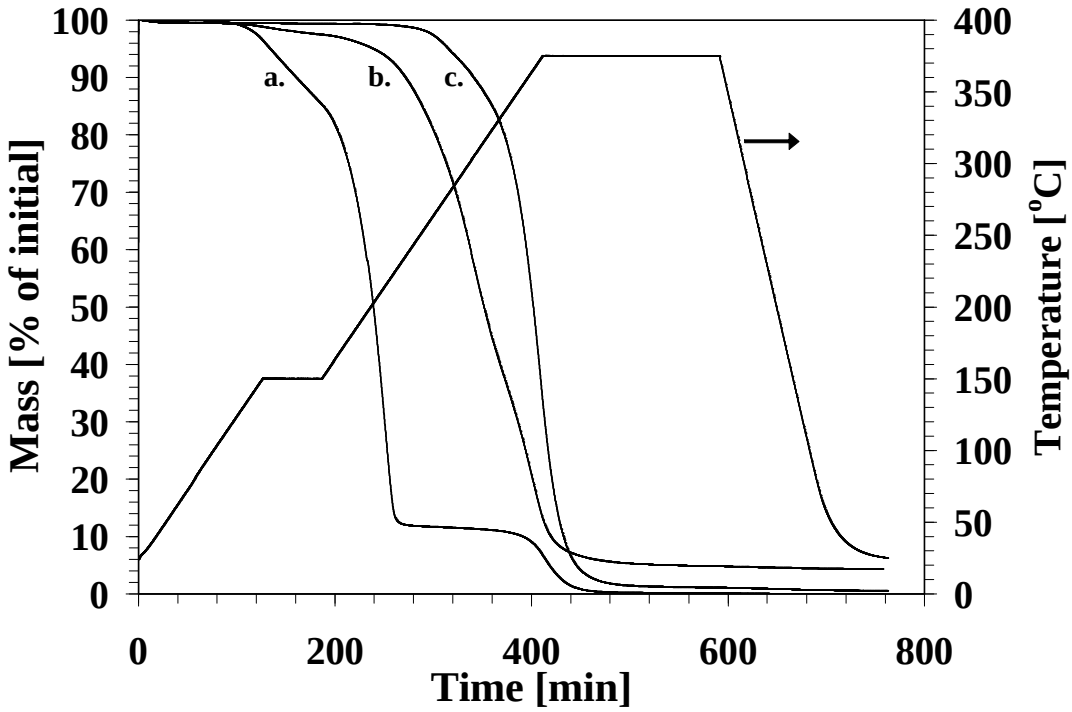

Figure 2: Thermogravimetric analysis (TGA) in flowing N_2 showing the weight loss versus time for the organic components used in tape casting the Cu and Mg powders: a) dibutyl phthalate, b) KD-1, and c) methyl methacrylate:ethyl acrylate. The thermal cycle, also shown, mimics the temperature profile used to remove the organics from the laminated tapes.

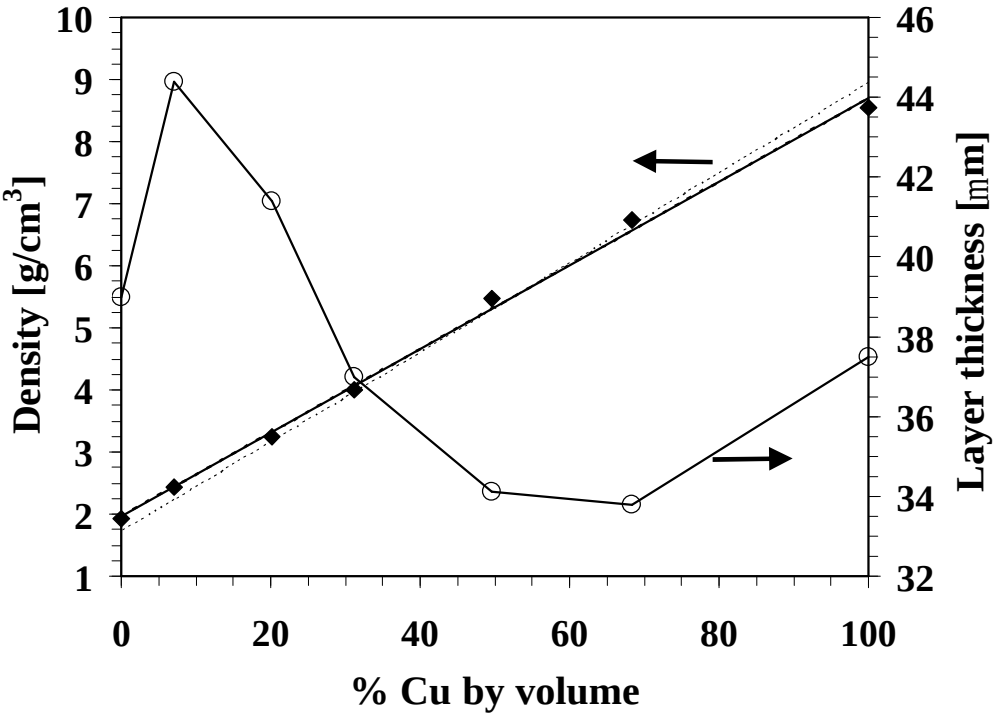

Figure 3: Density and layer thickness as a function of volume percent Cu for monolithic pellets fabricated by hot-pressing the tape cast Cu-Mg powder mixtures.

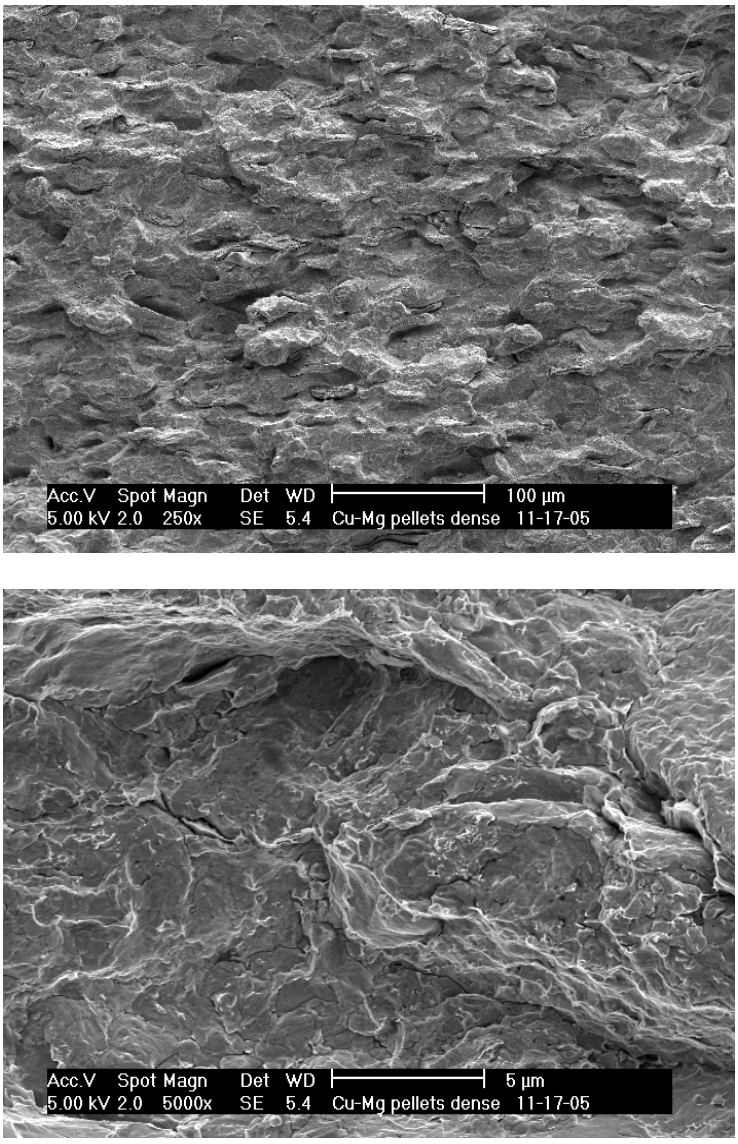

Figure 4: SEM micrographs of a fracture surface in a dense pellet fabricated from the 100% Cu tape (MC-1 in Table I).

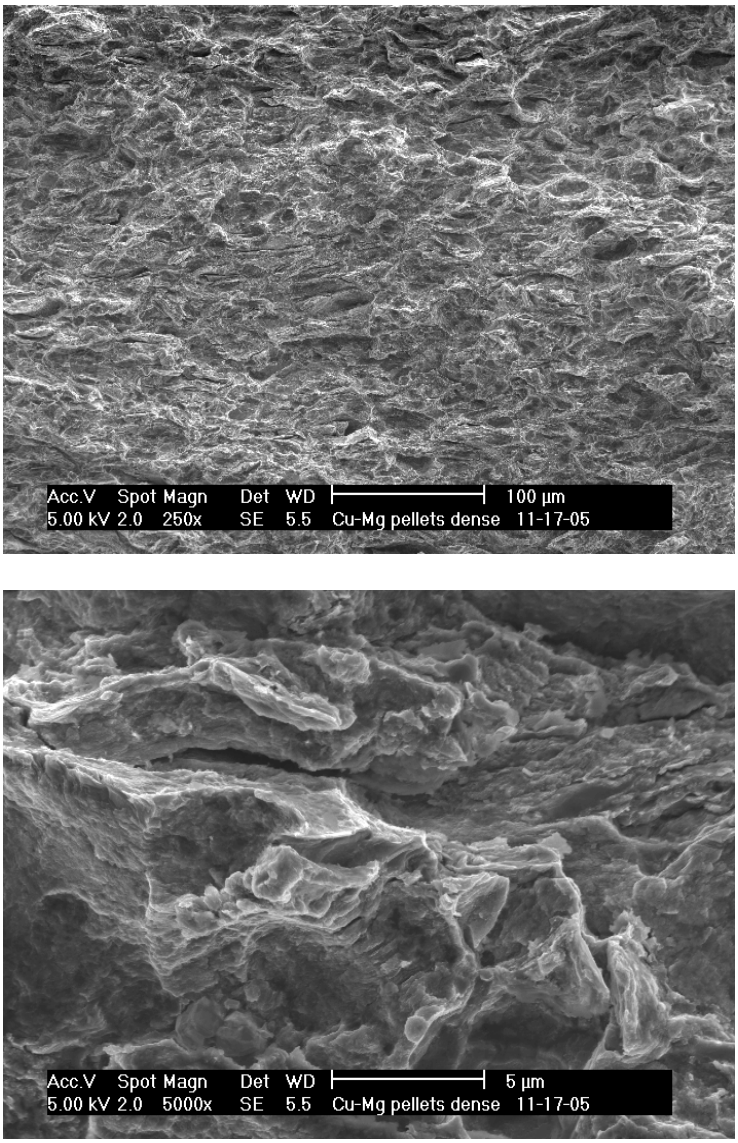

Figure 5: SEM micrographs of a fracture surface in a dense pellet fabricated from the 100% Mg tape (MC-7 in Table I).

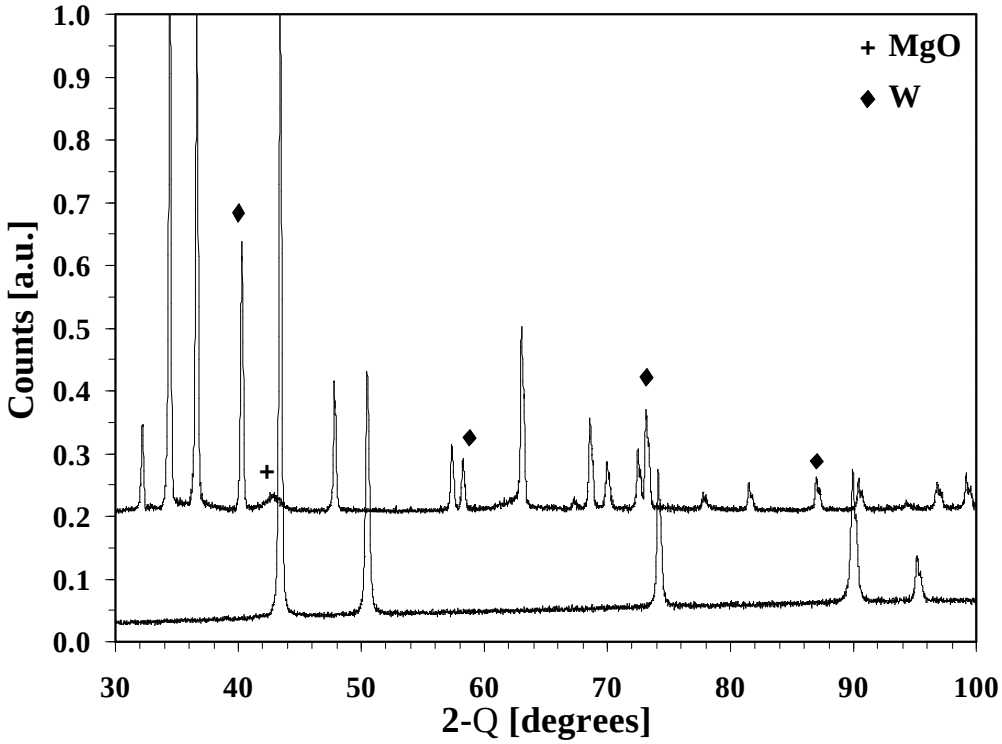

Figure 6: XRD patterns for the 100% Mg (upper curve) and 100% Cu (lower curve) compositions designated MC-1 and MC-7 in Table I.

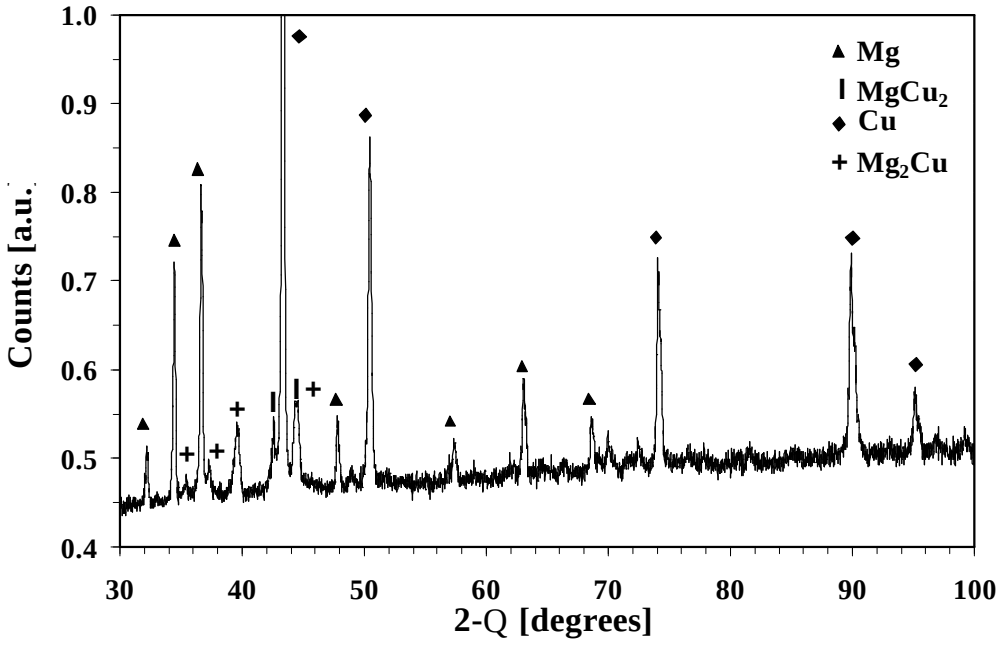

Figure 7a: XRD pattern for a dense pellet fabricated form MC-5 in Table I. The stoichiometry of the powder mixture corresponds to composition Mg_2Cu (67 atomic % Mg, 33 atomic % Cu).

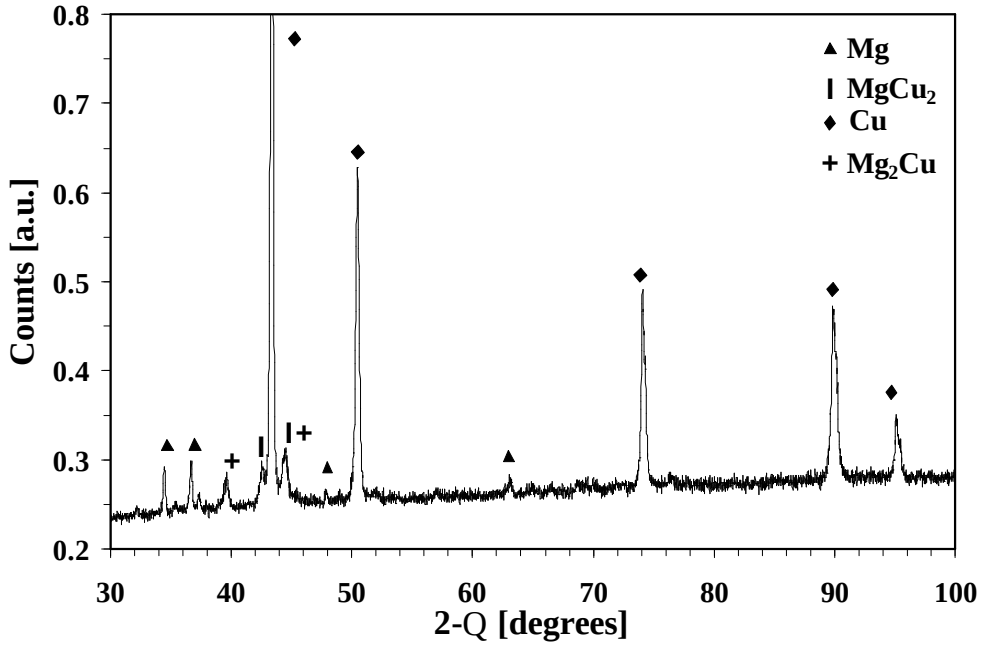

Figure 7b: XRD pattern for a dense pellet fabricated form MC-3 in Table I. The stoichiometry of the powder mixture corresponds to composition $MgCu_2$ (67 atomic % Cu, 33 atomic % Mg).

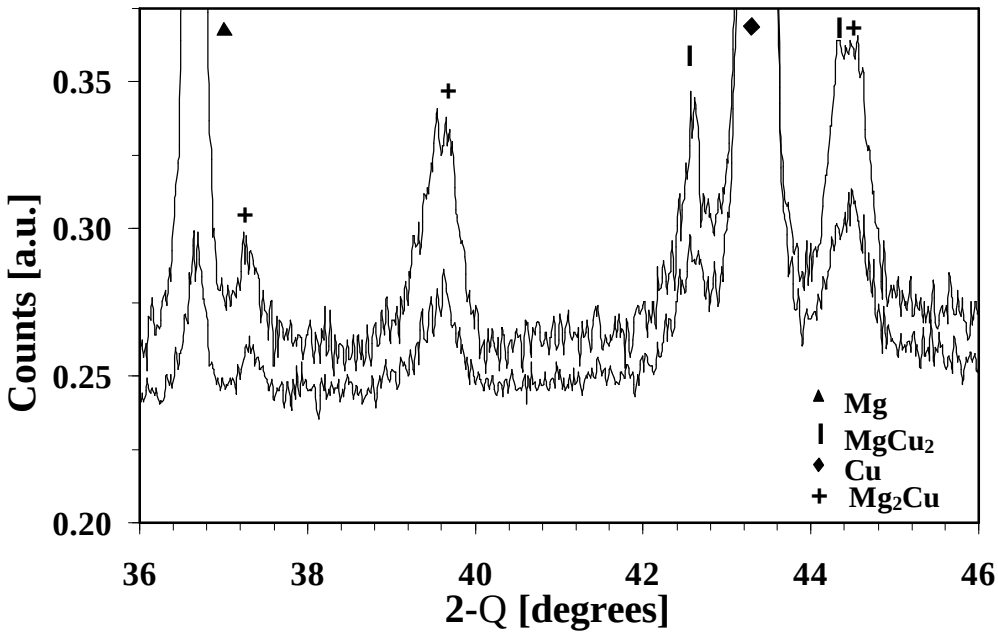

Figure 7c: Expanded view of the patterns in Figs. 7a and b showing the presence of both intermetallic phases $MgCu_2$ and Mg_2Cu for both compositions.

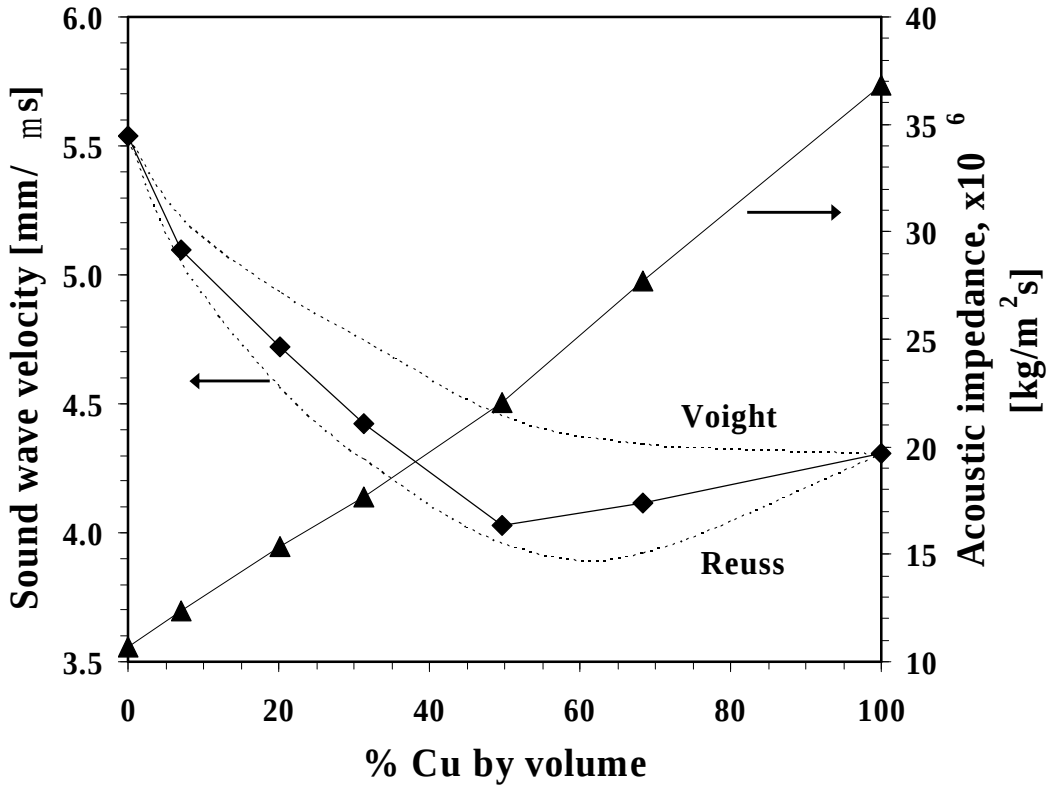

Figure 8: Longitudinal sound wave velocity and acoustic impedance as a function of volume percent Cu for monolithic pellets fabricated by hot-pressing the tape cast Cu-Mg powder mixtures.

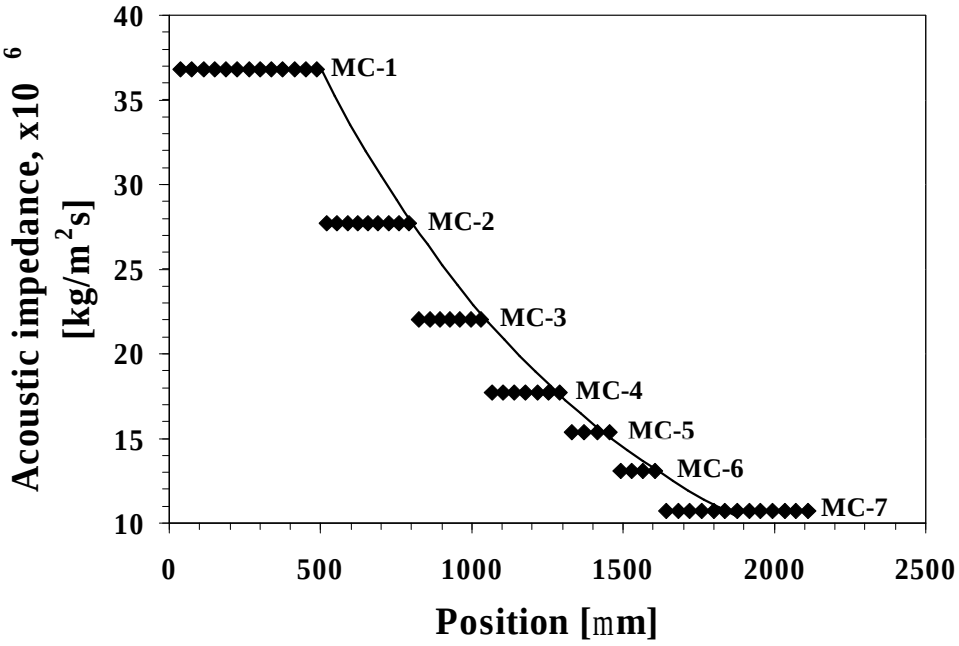

Figure 9: Target impedance profile and layer stacking sequence for a graded impactor fabricated from the tape cast Mg-Cu powders.

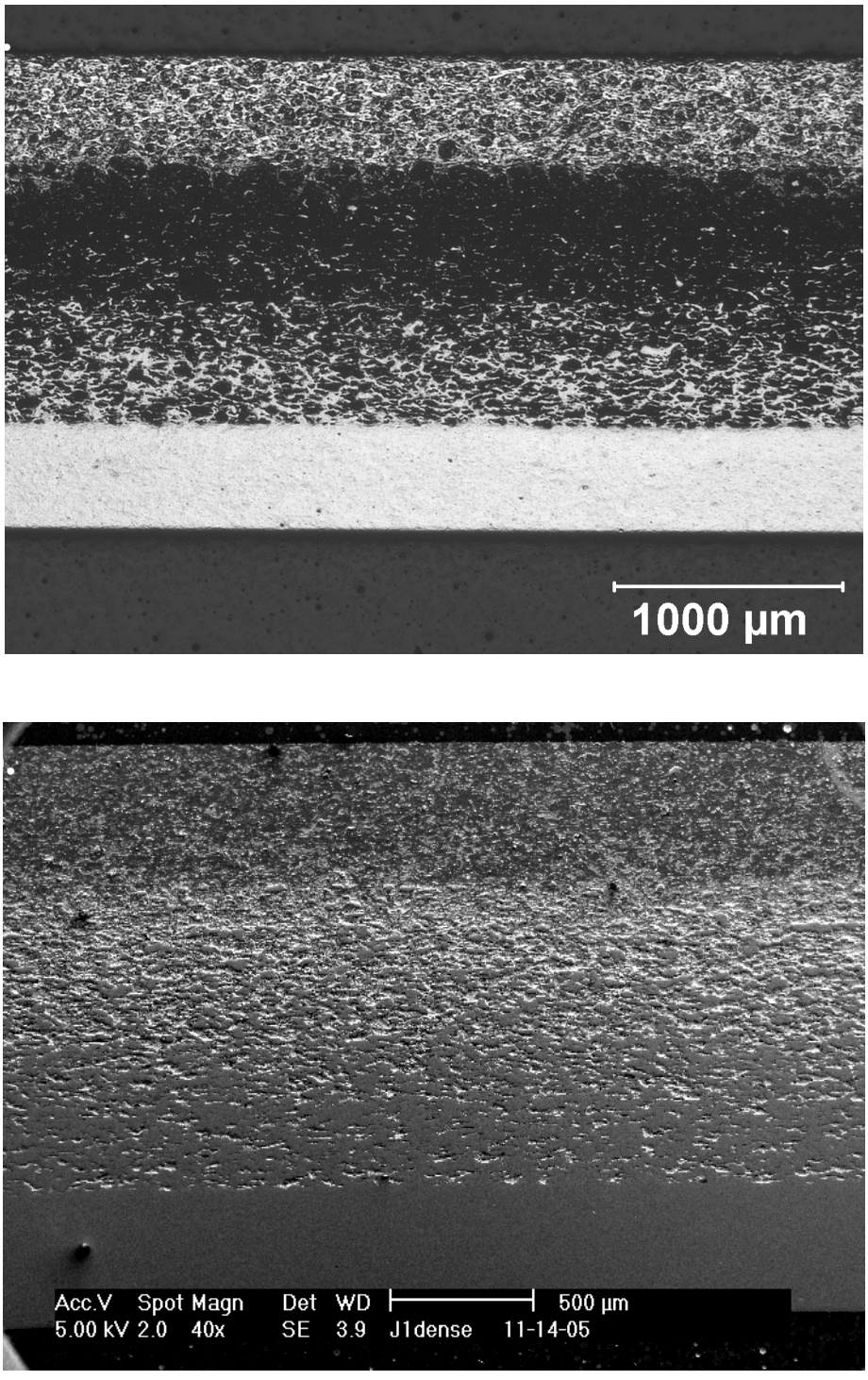

Figure 10: a) Optical, and b) SEM micrographs of a polished cross section of the graded impactor in Fig.9.

References

1. A.C. Mitchell and W.J. Nellis, J. App. Phys. 52, 3363 (1981).

2. J.H. Nguyen and N. C. Holmes, Nature 427, 339 (2004)

3. V. Iota, C.S. Yoo, and H. Cynn, Science 283, 1510 (1999).

4. H. Herberhold, S. Marchal, R. Lange, C.H. Scheyhing, R.F. Vogel, and R. Winter, J. Mol. Biol. 330, 1153 (2003).

5. V.V. Struzhkin, M.I. Eremets, W. Gan, H.-K. Mao, and R.J. Hemley, Science 298, 1213 (2002).

6. M. Eremets, High Pressure Experimental Methods (Oxford University Press, Oxford, 1996).

7. Y.B. Zel'dovich and Y.P. Raizer, Physics of Shock Waves and High-Temperature Hydrodynamic Phenomena (Academic Press, New York, 1967).

8. C.A. Hall, Phys. Plasma 7, 2069 (2000).

9. C.A. Hall, J.R. Assay, M.D. Knudsen, W.A.. Stygar, R.B. Spielman, T.D. Pointon, D.B. Reisman, A. Toor, and R.C. Cauble, Rev. Sci. Instrum. 72, 3587 (2001).

10. J. Edwards, K.T. Lorenz, B.A. Remington, S. Pollaine, J. Colvin, D. Braun, B.F. Lasinski, D. Reisman, J.M. McNaney, J.A. Greenough, R. Wallace, H. Louis, and D. Kalantar, Phys. Rev. Lett. 92, 75002/1 (2004).

11. J.H. Nguyen, D. Orlikowski, F.H. Streitz, J.A. Moriarty, and N.C. Holmes, submitted to J. Appl. Phys, (August, 2005).

12. J.H. Nguyen, D. Orlikowski, F.H. Streitz, J.A. Moriarty, N.C. Holmes, AIP Conf. Proc. 706, pt. 2, 1225 (2004).

13. Q. Shen, C.B. Wang, L.M. Zhang, J.S. Hua, H. Tan, F.Q. Jing, Key Eng. Mat. 249, 287 (2003).

14. H. Xiong, L.Zhang, L. Chen, R. Yuan, and T Hirai, Mat. Mat. Trans. 31A, 2369 (2000).

15. W.J. Nellis, S.T. Weir, and A.C. Mitchell, Phys. Rev. B 59, 3434 (1999).

16. Q. Shen, C.-B. Wang, L.-M. Zhang, J.-S. Hua, H. Tan, F.-Q. Jing, Acta Phys. Sinica 51, 1762 (2002).

17. L.M. Barker, Shock Waves Cond. Matt., J.R. Assay, R.A. Graham, and G.K. Straub, eds. (Elsevier, Amsterdam, 1984).

18. C. Wang, L. Zhang, and Q. Shen, Key Eng. Mat. 224-226, 489 (2002).

19. L. Zhang, Q. Shen, and Z. Yang, Mat. Sci. Forum 475-479, 1529 (2005).

20. B. Kieback, A. Neubrand, and H. Riedel, Mat. Sci. and Eng. A362, 81 (2003).

21. J.-G. Yeo, Y.-G. Jung, and S.-C. Choi, J. Eur. Ceram. Soc. 18, 1281 (1998).

22. Y.-P. Zheng, and D.-L. Jiang, J. Am. Ceram. Soc. 83, 2999 (2003).

23. R.M. German, Powder Metallurgy Science (MPIF, Princeton, NJ, 1994) p. 282.

24. A subsequent casting run was performed which yielded an uncontaminated, 100% Mg composition. Properties and performance where consistent between the two tapes except for the slightly elevated density (1.93g/cm^3) in the W-contaminated tape relative to the uncontaminated tape (1.81g/cm^3)

25. W. Koster and W. Rauscher, Technical Memorandum 1321 (National Advisory Committee for Aeronautics, Washington, D.C., 1951).

26. B. Arcot, Q.Z. Hong, W. Ziegler, and J.M.E. Harper, J. Appl. Phys. 76, 5161 (1994).

27. $MgCu_2$: JCPDF #013-0504, Mg_2Cu: JCPDF #001-1226.

28. J. Krautkramer and H. Krautkramer, Ultrasonic Testing of Materials (Springer-Verlag, New York, NY, 1990), p. 561.

29. Nondestructive Testing Handbook, Vol. 7, A.S. Birk, R.E. Green, and P. McIntire, eds.

(ASNT, Columbus, OH, 1991), pp. 836-840.

30. L. P. Martin, D. Dadon and M. Rosen, J. Am. Ceram. Soc. 79, 1281 (1996).

31. L. P. Martin, D. Nagle and M. Rosen, Mat. Sci. Eng. A246, 151 (1998).

32. T.K. Shen, P. Hing, J. Mat. Sci. 32, 6633 (1997).

33. W.D. Kingery, H.K. Bowen, and D.R. Uhlmann, Introduction to Ceramics (John Wiley & Sons, New York, NY, 1976), p. 774.

Figure captions

Table I: Composition and final (hot-pressed) density for the tape cast Mg – Cu powder mixtures. Also shown are the 'theoretical' densities predicted by Eq. (3), and the layer thickness for each tape composition.

Table II: Typical organic content for tape cast Mg – Cu powder mixtures. Specific formulations are dependant upon the density and specific surface area of the powder solids.

Table III: Measured characteristics of several graded impactors fabricated from the tape cast Mg - Cu powder mixtures. Values are expressed as the percentage of that predicted from the stacking sequence (Fig.) and the individual tape characteristics.

Figure 1: Flow chart illustrating the steps in a typical tape casting process.

Figure 2: Thermogravimetric analysis (TGA) in flowing N_2 showing the weight loss versus time for the organic components used in tape casting the Cu and Mg powders. The thermal cycle, also shown, mimics the temperature profile used to remove the organics from the laminated tapes.

Figure 3: Density and layer thickness as a function of volume percent Cu for monolithic pellets fabricated by hot-pressing the tape cast Cu-Mg powder mixtures.

Figure 4: SEM micrographs of a fracture surface in a dense pellet fabricated from the 100% Cu tape (MC-1 in Table I).

Figure 5: SEM micrographs of a fracture surface in a dense pellet fabricated from the 100% Mg tape (MC-7 in Table I).

Figure 6: XRD patterns for the 100% Mg (upper curve) and 100% Cu (lower curve) compositions designated MC-1 and MC-7 in Table I.

Figure 7a: XRD pattern for a dense pellet fabricated form MC-5 in Table I. The stoichiometry of the powder mixture corresponds to composition Mg_2Cu (67 atomic % Mg, 33 atomic % Cu).

Figure 7b: XRD pattern for a dense pellet fabricated form MC-3 in Table I. The stoichiometry of the powder mixture corresponds to composition $MgCu_2$ (67 atomic % Cu, 33 atomic % Mg).

Figure 7c: Expanded view of the patterns in Figs. 7a and b showing the presence of both intermetallic phases $MgCu_2$ and Mg_2Cu for both compositions.

Figure 8: Longitudinal sound wave velocity and acoustic impedance as a function of volume percent Cu for monolithic pellets fabricated by hot-pressing the tape cast Cu-Mg

powder mixtures.

Figure 9: Target impedance profile and layer stacking sequence for a graded impactor fabricated from the tape cast Mg-Cu powders.

Figure 10: Optical and SEM micrographs of the cross section of the graded impactor in Fig.7.